Bioorganic Chemistry 80 (2018) 525–530

Contents lists available at ScienceDirect

Bioorganic Chemistry

journal homepage: www.elsevier.com/locate/bioorg

Short communication

Bioactive secondary metabolites from the marine-associated fungus *Aspergillus terreus*

Mengting Liu[a,1], Weiguang Sun[a,1], Jianping Wang[a,1], Yan He[b], Jinwen Zhang[b], Fengli Li[a], Changxing Qi[a], Hucheng Zhu[a], Yongbo Xue[a], Zhengxi Hu[a,*], Yonghui Zhang[a,*]

[a] Hubei Key Laboratory of Natural Medicinal Chemistry and Resource Evaluation, School of Pharmacy, Tongji Medical College, Huazhong University of Science and Technology, Wuhan 430030, People's Republic of China
[b] Tongji Hospital, Tongji Medical College, Huazhong University of Science and Technology, Wuhan 430030, People's Republic of China

ARTICLE INFO

InChIKey:
JCFJNFBYQIPWAQ-RQNXDJOISA-N*Keywords:*
Marine-associated fungus
Aspergillus terreus
α-Glucosidase inhibition
Antibacterial
Anti-inflammatory
Molecular docking

ABSTRACT

Three new compounds, including a prenylated tryptophan derivative, luteoride E (**1**), a butenolide derivative, versicolactone G (**2**), and a linear aliphatic alcohol, (3*E*,7*E*)-4,8-dimethyl-undecane-3,7-diene-1,11-diol (**3**), together with nine known compounds (**4**–**12**), were isolated and identified from a coral-associated fungus *Aspergillus terreus*. Their structures were elucidated by HRESIMS, one- and two-dimensional NMR analysis, and the absolute configuration of **2** was determined by comparison of its electronic circular dichroism (ECD) spectrum with the literature. Structurally, compound **1** featured an unusual (*E*)-oxime group, which occurred rarely in natural products. Compounds **1**–**3** were evaluated for the α-glucosidase inhibitory activity, and compound **2** showed potent inhibitory potency with IC_{50} value of 104.8 ± 9.5 μM, which was lower than the positive control acarbose (IC_{50} = 154.7 ± 8.1 μM). Additionally, all the isolated compounds were evaluated for the anti-inflammatory activity against NO production, and compounds **1**–**3**, **5**–**7**, and **10** showed significant inhibitory potency with IC_{50} values ranging from 5.48 to 29.34 μM.

1. Introduction

With times moving rapidly, some new techniques and methods, such as synthetic biology [1], heterologous expression of gene clusters [2], OSMAC (One Strain/Many Compounds) [3], co-culture [3], etc., were successfully applied to explore the chemical space of terrestrial fungi, thus searching for new bioactive natural products from terrestrial fungi is becoming increasingly difficult. On the contrary, the ocean, which covers over 70% of the Earth's surface, is a neglected and insufficiently explored natural resource [4]. In recent years, the chemical investigations on marine organisms are increasing, of which many findings showed that marine-associated fungi are a prolific and promising resource of structurally novel and pharmaceutically active metabolites [5,6], including alkaloids, polyketides, terpenes, lignans, steroids, cyclic peptides, etc., with the surprising potentials for medicinal chemistry development, clinical trials and marketing.

Secondary metabolites that are produced by the *Aspergillus* species have attracted much attention from scientific community, because of their architecturally complex frameworks with multiple chiral centers and temping biological profiles. Representative examples included asperflavipine A [7], aspergilasines A–D [8], asperterpenes A and B [9], spiroaspertrione A [10], aspermerodione [11], and aspergillines A–E [12]. As part of our program to discover novel bioactive chemicals from marine-associated fungi [13–15], we performed a chemical investigation on a coral-associated fungus *Aspergillus terreus*, leading to the isolation and identification of three new compounds, including a prenylated tryptophan derivative, luteoride E (**1**), a butenolide derivative, versicolactone G (**2**), and a linear aliphatic alcohol, (3*E*,7*E*)-4,8-dimethyl-undecane-3,7-diene-1,11-diol (**3**), together with nine known compounds, which were identified as asterrelenin (**4**) [16], methyl 3,4,5-trimethoxy-2-(2-(nicotinamido)benzamido)benzoate (**5**) [17], 14α-hydroxyergosta-4,7,22-triene-3,6-dione (**6**) [18], territrem A (**7**) [19], territrem B (**8**) [20], territrem C (**9**) [20], lovastatin (**10**) [21], monacolin L acid methyl ester (**11**) [22], and monacolin L (**12**) [22] by detailed comparison of their NMR data and specific rotations with the literature. Remarkably, compound **1** featured an unusual (*E*)-oxime group, which occurred rarely in natural products. Herein, the details of the isolation, structural elucidation, and bioactivity evaluations of these compounds (Fig. 1) are described.

* Corresponding authors.
E-mail addresses: hzx616@126.com (Z. Hu), zhangyh@mails.tjmu.edu.cn (Y. Zhang).
[1] These authors contributed equally to this work.

https://doi.org/10.1016/j.bioorg.2018.06.029
Received 23 May 2018; Received in revised form 19 June 2018; Accepted 22 June 2018
Available online 27 June 2018

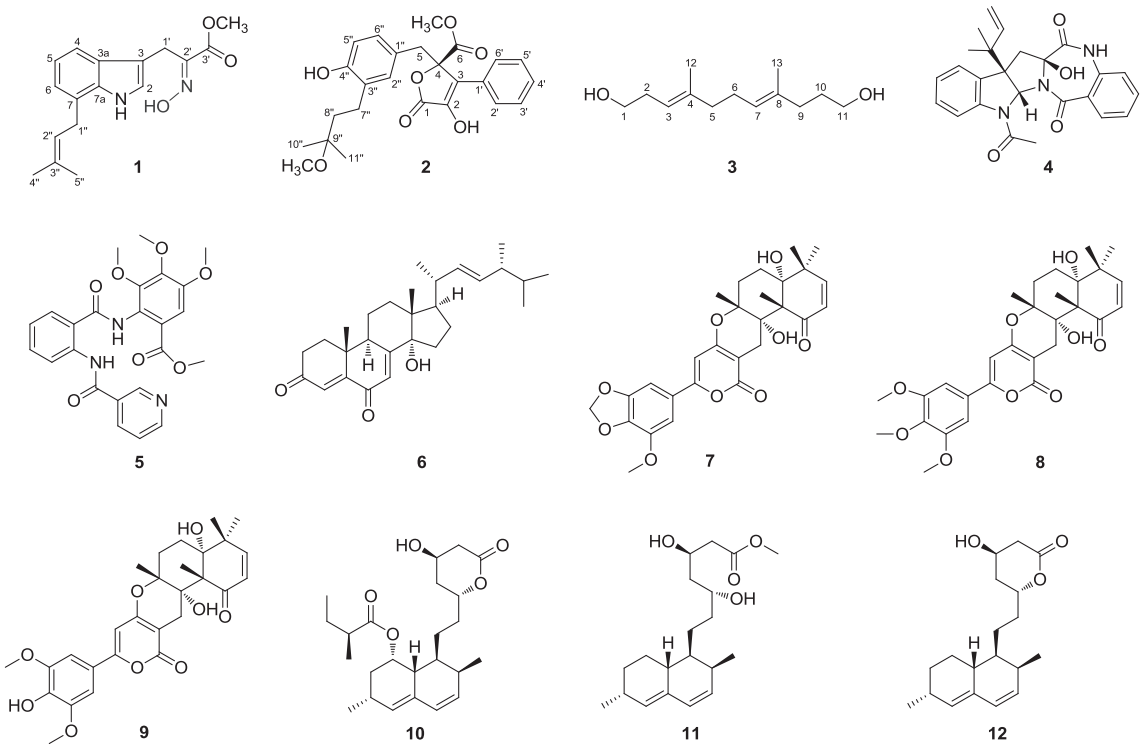

Fig. 1. Structures of compounds **1–12**.

2. Experiment

2.1. General

Optical rotations, UV, and FT-IR data were recorded on a PerkinElmer 341 instrument, a Varian Cary 50 instrument, and a Bruker Vertex 70 instrument with KBr pellets, respectively. ECD data were measured with a JASCO-810 CD spectrometer instrument. The high-resolution electrospray ionization mass spectra (HRESIMS) were recorded by using a positive ion mode on a Thermo Fisher LC-LTQ-Orbitrap XL instrument. One- and two-dimensional NMR data were recorded on a Bruker AM-400 instrument, with the reference of ^{1}H and ^{13}C NMR chemical shifts of the solvent peaks for methanol-d_4 (δ_H 3.31 and δ_C 49.0) and $CDCl_3$ (δ_H 7.24 and δ_C 77.23). Semi-preparative HPLC purifications were carried out by using an Agilent 1100 instrument with a Zorbax SB-C_{18} (9.4 mm × 250 mm) column. Column chromatography (CC) was carried out by using silica gel (200–300 mesh, Qingdao Marine Chemical, Inc., Qingdao, People's Republic of China), Lichroprep RP-C_{18} gel (40–63 μm, Merck, Darmstadt, Germany), and Sephadex LH-20 (GE Healthcare Bio-Sciences AB, Sweden). Silica gel 60 F_{254} and RP-C_{18} F_{254} plates were used for the TLC (thin-layer chromatography) detection, and spots were visualized by spraying heated silica gel plates with 10% H_2SO_4 in EtOH.

2.2. Fungal material

The strain *Aspergillus terreus* was separated from the coral *Sarcophyton subviride*, which was collected from the coast of Xisha Island in the South China Sea, in October 2016. For identification, this strain was cultured on potato dextrose agar (PDA) at 28 °C for a week in an incubator. The strain was identified based on its morphology analysis and ITS (Internal Transcribed Spacer) sequencing data of the rDNA. The ITS sequence data of this strain has been deposited at the GenBank (accession number MF972904). The fungal sample was deposited in the culture collection of Tongji Medical College, Huazhong University of Science and Technology.

2.3. Fermentation, extraction, and purification

The strain *Aspergillus terreus* was incubated on potato dextrose agar (PDA) medium at 28 °C for a week to prepare the seed cultures, which was then transferred into 300 × 500 mL Erlenmeyer flasks, each containing 200 g cooked rice. 28 days later, 300 mL EtOAc was added to each flask to stop the growth of cells, and followed by ultrasonic extraction with 95% aqueous EtOH at room temperature. Afterwards, the solvent was removed under reduced pressure to yield a total residue, which was then suspended in water and partitioned repeatedly with EtOAc (6 × 15 L). The EtOAc extract (1.5 kg) was chromatographed on silica gel CC using an increasing gradient of petroleum ether–ethyl acetate–MeOH (10:1:0, 7:1:0, 5:1:0, 3:1:0, 1:1:0, 2:2:1, 1:1:1) to afford seven fractions (A–G).

Fraction B (55 g) was chromatographed on silica gel CC (petroleum ether–ethyl acetate, 8:1–0:1, v/v) to yield three main fractions (B1–B3). Repeated purification of fraction B2 (4.6 g) using Sephadex LH-20 eluted with CH_2Cl_2–MeOH (1:1, v/v), RP-C_{18} column (MeOH–H_2O, from 30:70 to 100:0, v/v), and semi-preparative HPLC (isopropanol-*n*-hexane, 10:90, v/v, 2.0 mL/min) afforded compound **6** (t_R 12.2 min, 4.4 mg).

Fraction C (75 g) was subjected to an RP-C_{18} column eluted with MeOH–H_2O (from 20:80 to 100:0, v/v) to yield five fractions (C1–C5). Fraction C3 (2.3 g) was chromatographed on Sephadex LH-20 eluted with CH_2Cl_2–MeOH (1:1, v/v) to yield two fractions (C3.1–C3.2). Fraction C3.2 was further purified via repeated silica gel CC (stepwise petroleum ether–ethyl acetate, 4:1–1:1) to furnish three additional fractions (C3.2.1–C3.2.3). Purification of fraction C3.2.1 by using semi-preparative HPLC eluted with MeOH–H_2O (70:30, v/v, 3.0 mL/min) afforded compound **1** (t_R 27.2 min, 3.9 mg). Compound **2** (t_R 20.6 min, 4.5 mg) was purified by semi-preparative HPLC (MeOH–H_2O, 68:32, v/v, 3.0 mL/min) from fraction C3.2.2.

Fraction D (198 g) was separated by RP-C_{18} column with MeOH–H_2O (from 20:80 to 100:0, v/v) as eluent to yield five fractions (D1–D5) based on TLC analysis. Fraction D1 (45 g) was consecutively separated through Sephadex LH-20 eluted with CH_2Cl_2–MeOH (1:1, v/v) and silica gel CC

eluted with petroleum ether–ethyl acetate (3:1–1:1) to yield three fractions (D1.1–D1.3). Compound **4** (t_R 25.4 min, 15.1 mg) was purified by semi-preparative HPLC with MeCN − H_2O (55:45, v/v, 3.0 mL/min) from fraction D1.1. Fraction D1.2 was applied to semi-preparative HPLC with MeOH − H_2O (65:35, v/v, 3.0 mL/min) to afford compound **3** (t_R 24.5 min, 6.5 mg). Fraction D2 (70 g) was separated through Sephadex LH-20 eluted with CH_2Cl_2–MeOH (1:1, v/v) and silica gel CC using CH_2Cl_2 − MeOH (200:1–20:1, v/v) in a stepwise gradient of increasing polarity to yield four fractions (D2.1–D2.4). Purification of fraction D2.2 (3.5 g) using RP-C_{18} column with MeOH–H_2O (from 30:70 to 80:20, v/v), and followed by semi-preparative HPLC using MeCN − H_2O (55:45, v/v, 3.0 mL/min) afforded compound **8** (t_R 30.2 min, 5.5 mg). Fraction D2.3 (4.2 g) was further purified via a combination of RP-C_{18} column with MeOH–H_2O (from 20:80 to 80:20, v/v) and semi-preparative HPLC (MeOH − H_2O, 65:35, v/v, 3.0 mL/min) to give compound **7** (t_R 33.8 min, 40.5 mg). Compound **10** (163 mg) was purified from fraction D3 by crystallization from MeOH.

Fraction E (186 g) was chromatographed on silica gel CC (CH_2Cl_2–MeOH, 1:0–50:1, v/v) to yield five main fractions (E1–E5). Fraction E1 (2.6 g) was applied to RP-C_{18} column eluted with MeOH–H_2O (from 40:60 to 80:20, v/v) and followed by semi-preparative HPLC using MeOH–H_2O (75:25, v/v, 3.0 mL/min) to afford compounds **11** (t_R 54.1 min, 2.7 mg) and **12** (t_R 45.9 min, 4.6 mg). Repeated purification of fraction E2 using Sephadex LH-20 with MeOH as eluent, RP-C_{18} column (MeOH–H_2O, from 30:70 to 100:0, v/v), and semi-preparative HPLC (MeOH–H_2O, 60:40, v/v, 3.0 mL/min) afforded compounds **5** (48.8 mg, t_R 13.3 min) and **9** (17.7 mg, t_R 16.2 min).

2.4. Spectroscopic data

Compound **1**: yellow oil; UV (MeOH) λ_{max} (log ε) = 203 (4.51), 221 (4.57), 281 (3.81) nm; IR ν_{max} = 3423, 2923, 1726, 1631, 1440, 1383, 1345, 1210, 1081, 1024, 799, 748 cm^{-1}; HRESIMS *m/z* 301.1517 $[M+H]^+$ (calcd for $C_{17}H_{21}N_2O_3$, 301.1552) and *m/z* 323.1377 $[M+Na]^+$ (calcd for $C_{17}H_{20}N_2O_3Na$, 323.1372); For ^1H and ^{13}C NMR data, see Table 1.

Compound **2**: white, amorphous powders; $[\alpha]_{25}^{D}$: +81 (*c* 0.1, MeOH); UV (MeOH) λ_{max} (log ε) = 202 (4.62), 218 (4.15), 286 (4.14) nm; ECD (*c* 0.17, MeOH) $\Delta\varepsilon_{202}$ +27.80, $\Delta\varepsilon_{227}$ −7.11, $\Delta\varepsilon_{304}$ +2.94; IR ν_{max} = 3433, 2973, 2932, 2852, 1743, 1630, 1509, 1438, 1386, 1261, 1183, 1132, 1102, 1067, 1033, 764, 695 cm^{-1}; HRESIMS *m/z* 463.1708 $[M+Na]^+$ (calcd for $C_{25}H_{28}O_7Na$, 463.1733); For ^1H and ^{13}C NMR data, see Table 1.

Compound **3**: colorless oil; UV (MeOH) λ_{max} (log ε) = 202 (3.99) nm; IR ν_{max} = 3420, 2927, 1627, 1446, 1054, 675 cm^{-1}; HRESIMS *m/z* 213.1818 $[M+H]^+$ (calcd for $C_{13}H_{25}O_2$, 213.1855) and *m/z* 235.1644 $[M+Na]^+$ (calcd for $C_{13}H_{24}O_2Na$, 235.1674); For ^1H and ^{13}C NMR data, see Table 1.

2.5. In vitro α-glucosidase inhibition assay

The α-glucosidase enzyme was obtained from *Saccharomyces cerevisiae* (Sigma Aldrich, USA) and its solution (1.5 U/mL) was prepared by dissolving the α-glucosidase in 200 M phosphate buffer (pH 6.8). Then, the α-glucosidase enzyme solution (20 μL), test compounds (10 μL) and buffer (40 μL) were pipetted and mixed in a 96 well microtiter plate. After incubation at 37 °C for 10 min, *p*-nitrophenyl-α-D-glucopyranoside (PNP-G) substrate solution (10 μL, in 20 mM phosphate buffer) was added. The increment of absorbance due to the hydrolysis of PNP-G by α-glucosidase was measured at the wavelength of 410 nm with a microplate reader (Thermo Scientific, Waltham, MA). Acarbose was used as a positive control and averages of three replicates were calculated. The α-glucosidase inhibitory activity was expressed as percentage inhibition and was calculated using the following formula: inhibition (%) = $[1 - (OD_{sample}/OD_{blank})] \times 100\%$.

2.6. Molecular docking

The virtual docking was carried out in the Surflex-Dock module of the FlexX/Sybyl software, which belongs to a fast docking method that allows sufficient flexibility of ligands and keeps the target protein rigid. Molecules were built with Chemdraw software and further optimized at

Table 1
^1H and ^{13}C NMR data for compounds **1–3** (δ in ppm, *J* in Hz).

No.	**1** (in $CDCl_3$)		No.	**2** (in methanol-d_4)		No.	**3** (in methanol-d_4)	
	δ_H[a,b]	δ_C[c]		δ_H[a,b]	δ_C[c]		δ_H[a,b]	δ_C[c]
1	7.98 s	–	1	–	171.1 C	1	3.50 m	62.9 CH_2
2	7.08 s	123.4 CH	2	–	138.0 C	2	2.24 m	32.5 CH_2
3	–	110.0 C	3	–	126.5 C	3	5.16 m	121.6 CH
3a	–	127.4 C	4	–	87.1 C	4	–	138.1 C
4	7.61 d (7.9)	117.4 CH	5	3.47 d (11.5)	39.4 CH_2	5	2.02 m	40.8 CH_2
5	7.04 dd (7.0 and 7.9)	120.0 CH	6	–	171.7 C	6	2.11 m	27.5 CH_2
6	6.97 d (7.0)	121.8 CH	6-OMe	3.80 s	53.9 CH_3	7	5.14 m	125.5 CH
7	–	124.1 C	1′	–	132.4 C	8	–	135.7 C
7a	–	135.4 C	2′/6′	7.73 d (7.4)	128.4 CH	9	2.03 m	36.9 CH_2
1′	4.07 s	20.6 CH_2	3′/5′	7.45 dd (7.4 and 7.6)	129.8 CH	10	1.62 m	32.0 CH_2
2′	–	151.7 C	4′	7.36 dd (7.6 and 7.6)	129.4 CH	11	3.52 m	62.7 CH_2
3′	–	164.3 C	1″	–	125.2 C	12	1.64 s	16.2 CH_3
3′-OMe	3.77 s	52.9 CH_3	2″	6.41 d (1.9)	132.9 CH	13	1.61 s	16.0 CH_3
1″	3.51 d (7.2)	30.9 CH_2	3″	–	129.5 C			
2″	5.37 t (7.2)	122.4 CH	4″	–	155.3 C			
3″	–	133.5 C	5″	6.47 d (8.0)	115.2 CH			
4″	1.74 s	25.9 CH_3	6″	6.50 dd (1.9 and 8.0)	129.8 CH			
5″	1.78 s	18.2 CH_3	7″	2.29 m; 2.40 m	25.3 CH_2			
			8″	1.52 m	40.1 CH_2			
			9″	–	76.3 C			
			10″	1.16 s	25.6 CH_3			
			11″	1.16 s	25.6 CH_3			
			9″-OMe	3.18 s	49.5 CH_3			

[a] Recorded at 400 MHz.
[b] "m" means overlapped or multiplet with other signals.
[c] Recorded at 100 MHz.

molecular mechanical and semi-empirical level by Open Babel GUI. The crystallographic ligands were extracted from the active site and the designed ligands were modelled. All the hydrogen atoms were added to define the correct ionization and tautomeric states, and the carboxylate, phosphonate and sulphonate groups were considered in their charged form. In the docking calculation, the default FlexX scoring function was applied for exhaustive searching, solid body optimizing, and interaction scoring. Finally, the ligands with the lowest-energy and the most optimum orientation were chosen.

2.7. Antibacterial assay

The test strains were obtained from the ATCC: *Klebsiella pneumoniae* ATCC BAA2146, extended-spectrum *β*-lactamase-producing *Escherichia coli* ATCC 35218, and methicillin-resistant *Staphylococcus aureus* ATCC 43300. The antibacterial activities of compounds **1–3** were screened against these drug-resistant microbial pathogens according to the previously reported method [23].

2.8. Anti-inflammatory assay

RAW264.7 cells were seeded in 96-well cell culture plates (2×10^5 cells/well), each containing RPMI-1640 (Hyclone). After a 24 h pre-incubation, the seeded cells were treated with gradient dilutions of test compounds with a maxium concentration of 100 μM, followed by stimulation with LPS (1 μg/mL) for 18 h. NO production in the supernatant was assessed by the Griess reagent (Sigma). After a 5 min incubation, the absorbance at 570 nm was measured with a 2104 Envision multilabel plate reader (PerkinElmer Life Sciences, Inc., Boston, MA, USA). The inhibitor of proteasome, MG132, was used as a positive control.

$$\text{NO inhibitory (\%)} = (OD570_{treated} - OD570_{control})/OD570_{control} \times 100\%.$$

3. Results and discussion

3.1. Structure elucidation

Compound **1** was determined to have a molecular formula of $C_{17}H_{20}N_2O_3$, as deduced from the HRESIMS data at *m/z* 301.1517 $[M+H]^+$ (calcd for $C_{17}H_{21}N_2O_3$, 301.1552) and *m/z* 323.1377 $[M+Na]^+$ (calcd for $C_{17}H_{20}N_2O_3Na$, 323.1372), indicative of nine indices of hydrogen deficiency. The ^{13}C NMR and DEPT spectroscopic data (Table 1) of **1** revealed 17 carbon resonances that were attributed to two methyls at δ_C 18.2 and 25.9, two sp^3 methylenes at δ_C 20.6 and 30.9, five olefinic methines at δ_C 117.4, 120.0, 121.8, 122.4, and 123.4, six olefinic quaternary carbons at δ_C 110.0, 124.1, 127.4, 133.5, 135.4, and 151.7, one ester carbonyl at δ_C 164.3, and one methoxy group at δ_C 52.9. The ^1H NMR spectrum (Table 1) of **1** showed diagnostic signals for a 1,2,3-trisubstituted phenyl group at δ_H 7.61 (d, J = 7.9 Hz, H-4), 7.04 (dd, J = 7.0 and 7.9 Hz, H-5), and 6.97 (d, J = 7.0 Hz, H-6). With the aid of two ^1H NMR signals at δ_H 7.98 (s, NH-1) and 7.08 (s, H-2) and ^{13}C NMR data assigned to C-2–C-7, C-3a, and C-7a, it indicated the presence of a 3,7-disubstituted indole group. An isopentene group [δ_H 3.51 (d, J = 7.2 Hz, H_2-1″)/δ_C 30.9 (C-1″), δ_H 5.37 (t, J = 7.2 Hz, H-2″)/δ_C 122.4 (C-2″), δ_C 133.5 (C-3″), δ_H 1.74 (s, H_3-4″)/δ_C 25.9 (C-4″), and δ_H 1.78 (s, H_3-5″)/δ_C 18.2 (C-5″)] was located at C-7 based on the ^1H–^1H COSY correlation of H_2-1″/H-2″ and HMBC correlations from H_3-4″ to C-2″, C-3″, and C-5″ and from H_2-1″ to C-6, C-7, and C-7a. In the HMBC experiment (Fig. 2), the methoxy signal at δ_H 3.77 correlated with an ester carbonyl at δ_C 164.3, suggesting the presence of a methyl ester group. Except for these attributive signals, only two carbon resonances at δ_C 20.6 and 151.7 were remaining, thus, we deduced that a C=NOH group should exist, as supported by its molecular formula $C_{17}H_{20}N_2O_3$ required by the HRESIMS data. The HMBC correlations from H_2-1′ (δ_H 4.07) to C-2, C-3, C-3a, C-2′, and C-3′ suggested the methyl 2-(hydroxyimino)propanoate group was attached at C-3. Thus, the planar structure of **1** was determined (Fig. 2).

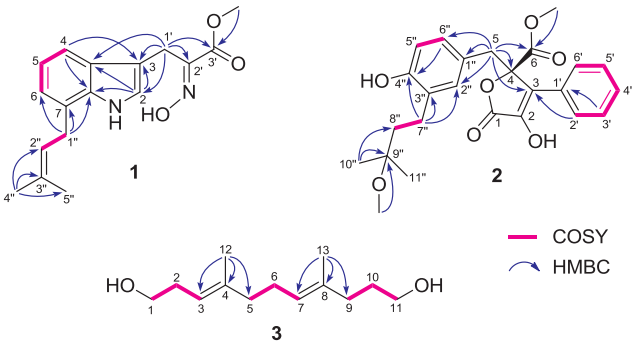

Fig. 2. Selected ^1H–^1H COSY and HMBC correlations of **1–3**.

By comparison of the ^{13}C NMR data of **1** with those of luteoride A [24], which was also a rare tryptophan derivative with an unusual methyl 2-(hydroxyimino)propanoate group, the nearly identical NMR data [δ_C 123.4 (CH, C-2), 110.0 (C, C-3), 20.6 (CH_2, C-1′), 151.7 (C, C-2′), and 164.3 (C, C-3′) for **1**; δ_C 123.5 (CH, C-2), 109.8 (C, C-3), 20.2 (CH_2, C-1′), 151.0 (C, C-2′), and 164.3 (C, C-3′) for luteoride A] indicated that the geometry of the oxime moiety in **1** was established as *E*-from. Accordingly, the stereochemistry structure of **1** was defined and named luteoride E.

Compound **2** was obtained as a white, amorphous powder and showed a molecular formula of $C_{25}H_{28}O_7$, on the basic of its HRESIMS analysis at *m/z* 463.1708 $[M+Na]^+$ (calcd for $C_{25}H_{28}O_7Na$, 463.1733), requiring twelve indices of hydrogen deficiency. The IR spectrum of **2** exhibited characterized absorption bands for hydroxy group (3433 cm^{-1}), ester/lactone carbonyl group (1743 cm^{-1}), and aromatic rings (1630 and 1509 cm^{-1}). In the ^1H NMR spectrum (Table 1) of **2**, the signals of a mono-substituted benzene motif at δ_H 7.73 (2H, d, J = 7.4 Hz, H-2′, 6′), δ_H 7.45 (2H, dd, J = 7.4 and 7.6 Hz, H-3′, 5′), and δ_H 7.36 (1H, dd, J = 7.6 and 7.6 Hz, H-4′), a 1,3,4-trisubstituted benzene motif at δ_H 6.41 (1H, d, J = 1.9 Hz, H-2″), 6.47 (1H, d, J = 8.0 Hz, H-5″), and 6.50 (1H, dd, J = 1.9 and 8.0 Hz, H-6″), and two methoxy protons at δ_H 3.18 (3H, s, OMe-9″) and 3.80 (3H, s, OMe-6) were clearly observed. The ^{13}C NMR and DEPT data suggested the presence of four sp^3 methyls (including two oxygenated ones), three sp^3 methylenes, eight sp^2 methines, and ten quaternary carbons (including six sp^2 ones, two oxygenated ones, and two carbonyl groups). Among these functionalities, two carbonyls and fourteen olefinic carbons occupied nine out of twelve indices of hydrogen deficiency. These data above suggested that compound **2** was a butenolide derivative.

Close comparison of the ^1H and ^{13}C NMR data (Table 1) of **2** with those of versicolactone B [25], which was evidenced via crystallography experiment, indicated that both compounds shared the same basic skeleton, with the only difference being that the $\Delta^{8'',9''}$ double bond in versicolactone B was replaced by an sp^3 methylene carbon (δ_C 40.1, C-8″) and an oxygenated tertiary carbon (δ_C 76.3, C-9″) with the attachment of a methoxy group (δ_C 49.5, OMe-9″) in **2**, as supported via the HMBC correlations from H_3-10″ to C-8″ and C-9″ and from the methoxy proton (δ_H 3.18) to C-9″. The gross structure of **2** was further confirmed by the ^1H–^1H COSY and HMBC correlations as shown in Fig. 2.

To determine the absolute configuration of C-4, the experimental ECD curve of **2** was measured in MeOH (Fig. 3), which was consistent with that of versicolactone B [25], displaying positive Cotton effects at nearly 202 and 304 nm and a negative Cotton effect at nearly 227 nm that owned to the chromophore of an *α*,*β*-unsaturated carboxylic ester group conjugated to a benzene group. Accordingly, compound **2** was deduced to be 4*R*-configuration and named versicolactone G.

Compound **3** was obtained as colorless oil. Its molecular formula was determine to be $C_{13}H_{24}O_2$, based upon the HRESIMS analysis at *m/*

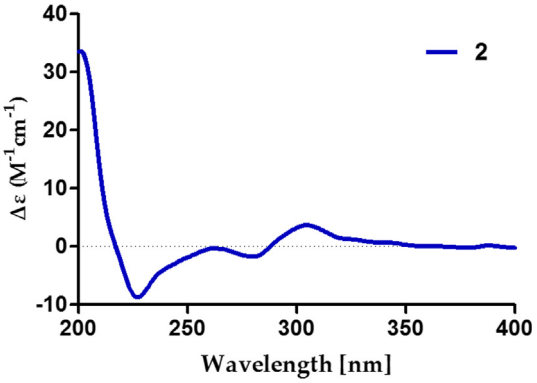

Fig. 3. Experimental ECD spectrum of compound **2**.

z 213.1818 $[M+H]^+$ (calcd for $C_{13}H_{25}O_2$, 213.1855) and *m/z* 235.1644 $[M+Na]^+$ (calcd for $C_{13}H_{24}O_2Na$, 235.1674), corresponding to two indices of hydrogen deficiency. In its ^1H NMR spectrum (Table 1), two olefinic protons at δ_H 5.14 (m, H-7) and 5.16 (m, H-3), two oxygenated methylenes at δ_H 3.50 (m, H_2-1) and 3.52 (m, H_2-11), and two methyls at δ_H 1.61 (s, H_3-13) and 1.64 (s, H_3-12) were observed. Its ^{13}C NMR and DEPT data revealed the presence of two sp^3 methyls, seven sp^3 methylenes (including two oxygenated ones), two sp^2 methines, and two sp^2 quaternary carbons. The presence of four olefinic carbons occupied two out of two indices of hydrogen deficiency, suggesting that compound **3** was a linear aliphatic alcohol.

The key 2D NMR spectra (Fig. 2), including ^1H–^1H COSY correlations of H_2-1/H_2-2/H-3, H_2-5/H_2-6/H-7, and H_2-9/H_2-10/H_2-11 and HMBC correlations from H_3-12 to C-3, C-4, and C-5 and from H_3-13 to C-7, C-8, and C-9 confirmed the planar structure of **3**. Based on the key NOESY correlations of H-3/H_2-5 and H-7/H_2-9 (Fig. S25, Supporting Information), the C-3–C-4 and C-7–C-8 double bonds were determined to be *E*-geometries. Accordingly, the structure of **3** was defined and named (3*E*,7*E*)-4,8-dimethyl-undecane-3,7-diene-1,11-diol.

3.2. Biological activity assessment

Compounds **1–3** were evaluated for the *α*-glucosidase inhibitory activity (Table 2), and compound **2** showed potent inhibitory potency with IC_{50} value of 104.8 ± 9.5 μM, which was lower than the positive control acarbose (IC_{50} = 154.7 ± 8.1 μM). To further investigate the binding mode of **2** with *α*-glucosidase, molecular docking study was carried out by using SYBYL 2.0 software. Due to the unavailable of crystal structure of *α*-glucosidase from *Saccharomyces cerevisiae*, the crystal structure of isomaltase (PDB ID: 3A4A) from *S. cerevisiae*, which is 84% similar to that of *S. cerevisiae α*-glucosidase was conducted as docking model [26]. The calculated binding modes of **2** in the potential active site were illustrated in Fig. 4 (A and B). Compound **2** could be deeply buried into the binding pocket which was located at the rim of the substrate-binding site. Detailed analysis further showed that the benzene group of **2** formed π-π stacking interaction with the residue Phe303. It was also shown that the residue Asp215, Glu411 and Arg442

Table 2
α-Glucosidase inhibitory activity of compounds **1–3**.

No.	IC_{50} (*μ*M) *α*-glucosidase inhibitory activity[b]
1	> 200
2	104.8 ± 9.5
3	> 200
Acarbose[a]	154.7 ± 8.1

[a] Acarbose was used as the positive control.
[b] Data were represented as the mean ± SD of three triplicate experiments.

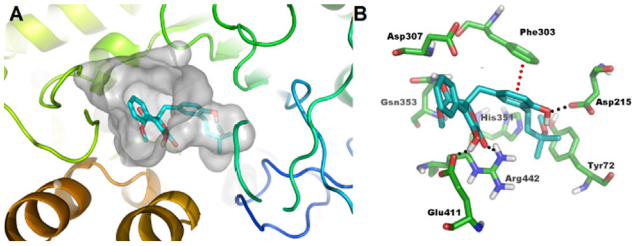

Fig. 4. Low-energy binding conformations of compound **2** bound to the target generated by virtual ligand docking. The key hydrogen and π-π bonding interactions of **2** to the enzyme is shown with the black and red balls, respectively.

formed key hydrogen bonds with **2**. Therefore, **2** was capable of inhibiting *α*-glucosidase by binding in the active site through key π-π interaction and multiple hydrogen bonds in a cooperative way.

Furthermore, compounds **1–3** were screened for antibacterial activities against three drug-resistant microbial pathogens (*Klebsiella pneumonia*, extended-spectrum *β*-lactamase-producing *Escherichia coli*, and methicillin-resistant *Staphylococcus aureus*); unfortunately, none of them exhibited significant activities with MIC values of > 100 μg/mL. Additionally, in our continuous screening for anti-inflammatory agents from natural product library [27], all the isolates **1–12** were evaluated for the anti-inflammatory activity against NO production. Among them (Table 3), compounds **1–3**, **5–7**, and **10** showed significant inhibitory potency with IC_{50} values ranging from 5.48 to 29.34 μM.

4. Concluding remarks

In conclusion, three new compounds, including a prenylated tryptophan derivative, luteoride E (**1**), a butenolide derivative, versicolactone G (**2**), and a linear aliphatic alcohol, (3*E*,7*E*)-4,8-dimethyl-undecane-3,7-diene-1,11-diol (**3**), together with nine known compounds (**4–12**), were isolated from a coral-associated fungus *Aspergillus terreus*. Remarkably, Li and co-workers have systematically investigated the enzyme assays of prenylated tryptophan derivatives [28–32], wherein the FgaPT2 and 7-DMATS from *Aspergillus fumigatus* and 5-DMATS from *Aspergillus clavatus* catalyzed prenylation of L-tryptophan at C-4, C-7, and C-5, respectively. To our knowledge, despite compound **1** belonged to a structural analogue, it featured an unusual (*E*)-oxime group, which occurred rarely in natural products and represented the first example of oxime-containing prenylated tryptophan derivative in the *Aspergillus* species. In addition, the benzyl- and phenyl-disubstituted γ-butenolides, which could be classified as 2,3-, 2,4-, and 3,4-disubstituted γ-butenolides according to the substituted patterns of lactone core [33], were commonly found in the *Aspergillus* species, such as *Aspergillus flavipes* [33], *Aspergillus terreus* [34], *Aspergillus versicolor* [25], etc. Structurally, compound **2** belonged to the typical 3,4-disubstituted γ-butenolide, and it featured a distinctive methoxy group linked to C-9″ in the C-3″ isopentane side chain [25]. Compound **2** showed potent *α*-glucosidase inhibitory potency with IC_{50} value of 104.8 ± 9.5 μM, which was

Table 3
Inhibitory activity against LPS-induced NO production of **1–12**.

No.	IC_{50} (μM) NO production	No.	IC_{50} (μM) NO production
1	24.64	**7**	29.34
2	15.72	**8**	> 40
3	18.62	**9**	> 40
4	> 40	**10**	17.45
5	5.48	**11**	> 40
6	26.83	**12**	> 40
MG132[a]	0.24		

[a] MG132 was used as the positive control.

lower than the positive control acarbose (IC_{50} = 154.7 ± 8.1 μM). Additionally, compounds **1–3**, **5–7**, and **10** showed significant anti-inflammatory activity against NO production with IC_{50} values in the range of 5.48–29.34 μM. Our findings have demonstrated the huge potentials of coral-associated fungi for the discovery of structurally novel and pharmacologically active natural products.

Acknowledgments

We thank the Analytical and Testing Center at HUST for ECD and IR analyses. The generous supports from the Innovative Research Groups of the National Natural Science Foundation of China (No. 81721005), the National Natural Science Foundation of China (Nos. 81573316, 21702067, 81502943, and 81703580), the Program for Changjiang Scholars of Ministry of Education of the People's Republic of China (No. T2016088), the National natural Science Foundation for Distinguished Young Scholars (No. 81725021), the China Postdoctoral Science Foundation Funded Project (Nos. 2017M610479 and 2018T110777), and Hubei Provincial Natural Science Foundation of China (No. 2018CFB152) are greatly acknowledged.

Conflict of interest

The authors of the present manuscript have declared that no competing interests exist.

Appendix A. Supplementary material

Supplementary data associated with this article can be found, in the online version, at https://doi.org/10.1016/j.bioorg.2018.06.029. These data include MOL files and InChiKeys of the most important compounds described in this article.

References

[1] S. Ausländer, D. Ausländer, M. Fussenegger, Angew. Chem. Int. Ed. 56 (2017) 6396–6419.
[2] F. Alberti, G.D. Foster, A.M. Bailey, Appl. Microbiol. Biotechnol. 101 (2017) 493–500.
[3] S. Kusari, C. Hertweck, M. Spiteller, Chem. Biol. 19 (2012) 792–798.
[4] K. Sueyoshi, A. Yamano, K. Ozaki, S. Sumimoto, A. Iwasaki, K. Suenaga, T. Teruya, Mar. Drugs 15 (2017) 367–379.
[5] L. Jin, C. Quan, X. Hou, S. Fan, Mar. Drugs 14 (2016) 76–100.
[6] J.F. Imhoff, Mar. Drugs 14 (2016) 19–37.
[7] H. Zhu, C. Chen, Q. Tong, J. Yang, G. Wei, Y. Xue, J. Wang, Z. Luo, Y. Zhang, Angew. Chem. Int. Ed. 56 (2017) 5242–5246.
[8] G. Wei, C. Chen, Q. Tong, J. Huang, W. Wang, Z. Wu, J. Yang, J. Liu, Y. Xue, Z. Luo, J. Wang, H. Zhu, Y. Zhang, Org. Lett. 19 (2017) 4399–4402.
[9] C. Qi, J. Bao, J. Wang, H. Zhu, Y. Xue, X. Wang, H. Li, W. Sun, W. Gao, Y. Lai, J.G. Chen, Y. Zhang, Chem. Sci. 7 (2016) 6563–6572.
[10] Y. He, Z. Hu, W. Sun, Q. Li, X.N. Li, H. Zhu, J. Huang, J. Liu, J. Wang, Y. Xue, Y. Zhang, J. Org. Chem. 82 (2017) 3125–3131.
[11] Y. Qiao, X. Zhang, Y. He, W. Sun, W. Feng, J. Liu, Z. Hu, Q. Xu, H. Zhu, J. Zhang, Z. Luo, J. Wang, Y. Xue, Y. Zhang, Sci. Rep. 8 (2018) 5454–5464.
[12] M. Zhou, M.M. Miao, G. Du, X.N. Li, S.Z. Shang, W. Zhao, Z.H. Liu, G.Y. Yang, C.T. Che, Q.F. Hu, X.M. Gao, Org. Lett. 16 (2014) 5016–5019.
[13] Z.X. Hu, Y.B. Xue, X.B. Bi, J.W. Zhang, Z.W. Luo, X.N. Li, G.M. Yao, J.P. Wang, Y.H. Zhang, Mar. Drugs 12 (2014) 5563–5575.
[14] B. Yang, W. Sun, J. Wang, S. Lin, X.N. Li, H. Zhu, Z. Luo, Y. Xue, Z. Hu, Y. Zhang, Mar. Drugs 16 (2018) 110–118.
[15] M. Liu, Q. Zhou, J. Wang, J. Liu, C. Qi, Y. Lai, H. Zhu, Y. Xue, Z. Hu, Y. Zhang, RSC Adv. 8 (2018) 13040–13047.
[16] G.Y. Li, B.G. Li, T. Yang, J.H. Yin, H.Y. Qi, G.Y. Liu, G.L. Zhang, J. Nat. Prod. 68 (2005) 1243–1246.
[17] Y. Wang, J. Zheng, P. Liu, W. Wang, W. Zhu, Mar. Drugs 9 (2011) 1368–1378.
[18] P. Bladon, T. Sleigh, J. Chem. Soc. (1965) 6991–7000.
[19] S.S. Lee, J. Nat. Prod. 55 (1992) 251–255.
[20] X.H. Nong, Y.F. Wang, X.Y. Zhang, M.P. Zhou, X.Y. Xu, S.H Qi, Mar. Drugs 12 (2014) 6113–6124.
[21] P. Phainuphong, V. Rukachaisirikul, S. Saithong, S. Phongpaichit, K. Bowornwiriyapan, C. Muanprasat, C. Srimaroeng, A. Duangjai, J. Sakayaroj, J. Nat. Prod. 79 (2016) 1500–1507.
[22] J. Ma, Y. Li, Q. Ye, J. Li, Y. Hua, D. Ju, D. Zhang, R. Cooper, M. Chang, J. Agric. Food Chem. 48 (2000) 5220–5225.
[23] Y. He, Z. Hu, Q. Li, J. Huang, X.N. Li, H. Zhu, J. Liu, J. Wang, Y. Xue, Y. Zhang, J. Nat. Prod. 80 (2017) 2399–2405.
[24] T. Asai, T. Yamamoto, Y. Oshima, Tetrahedron Lett. 52 (2011) 7042–7045.
[25] M. Zhou, G. Du, H.Y. Yang, C.F. Xia, J.X. Yang, Y.Q. Ye, X.M. Gao, X.N. Li, Q.F. Hu, Planta Med. 81 (2015) 235–240.
[26] X. Shen, W. Saburi, Z. Gai, K. Kato, T. Ojima-Kato, J. Yu, K. Komoda, Y. Kido, H. Matsui, H. Mori, M. Yao, Acta Cryst. 71 (2015) 1382–1391.
[27] Z. Hu, Y. Wu, S. Xie, W. Sun, Y. Guo, X.N. Li, J. Liu, H. Li, J. Wang, Z. Luo, Y. Xue, Y. Zhang, Org. Lett. 19 (2017) 258–261.
[28] P. Mai, G. Zocher, L. Ludwig, T. Stehle, S.M. Li, Adv. Synth. Catal. 358 (2016) 1639–1653.
[29] M. Liebhold, X. Xie, S.M. Li, Org. Lett. 14 (2012) 4882–4885.
[30] J. Winkelblech, M. Liebhold, J. Gunera, X. Xie, P. Kolb, S.M. Li, Adv. Synth. Catal. 357 (2015) 975–986.
[31] A. Kremer, S.M. Li, Appl. Microbiol. Biotechnol. 79 (2008) 951–961.
[32] A. Fan, S.M. Li, Tetrahedron Lett. 55 (2014) 5199–5202.
[33] C. Wang, L. Guo, J. Hao, L. Wang, W. Zhu, J. Nat. Prod. 79 (2016) 2977–2981.
[34] Y. Sun, J. Liu, L. Li, C. Gong, S. Wang, F. Yang, H. Hua, H. Lin, Bioorg. Med. Chem. Lett. 28 (2018) 315–318.